TRANSACTIONS OF THE
AMERICAN MATHEMATICAL SOCIETY
Volume 356, Number 1, Pages 283–289
S 0002-9947(03)03230-6
Article electronically published on August 25, 2003

EMBEDDED MINIMAL DISKS: PROPER VERSUS NONPROPER—GLOBAL VERSUS LOCAL

TOBIAS H. COLDING AND WILLIAM P. MINICOZZI II

Abstract. We construct a sequence of compact embedded minimal disks in a ball in $\mathbf{R}^3$ with boundaries in the boundary of the ball and where the curvatures blow up only at the center. The sequence converges to a limit which is not smooth and not proper. If instead the sequence of embedded disks had boundaries in a sequence of balls with radii tending to infinity, then we have shown previously that any limit must be smooth and proper.

0. Introduction

Consider a sequence of compact embedded minimal disks $\Sigma_i \subset B_{R_i} = B_{R_i}(0) \subset \mathbf{R}^3$ with $\partial\Sigma_i \subset \partial B_{R_i}$ and either

(a) R_i equal to a finite constant, or

(b) $R_i \to \infty$.

We will refer to (a) as the *local case* and to (b) as the *global case*. Recall that a surface $\Sigma \subset \mathbf{R}^3$ is said to be properly embedded if it is embedded and the intersection of Σ with any compact subset of $\mathbf{R}^3$ is compact. We say that a lamination or foliation is proper if each leaf is proper.

We will be interested in the possible limits of sequences of minimal disks Σ_i as above where the curvatures blow up, e.g., $\sup_{B_1 \cap \Sigma_i} |A|^2 \to \infty$ as $i \to \infty$. In the global case, Theorem 0.1 in [CM2] gives a subsequence converging off a Lipschitz curve to a foliation by parallel planes; cf. Figure 1. In particular, the limit is a (smooth) foliation which is proper. We show here in Theorem 1 that smoothness and properness of the limit can fail in the local case; cf. Figure 2.

We will need the notion of a multi-valued graph; see Figure 3. Let $D_r \subset \mathbf{C}$ be the disk in the plane centered at the origin and of radius r, and let $\mathcal{P}$ be the universal cover of the punctured plane $\mathbf{C} \setminus \{0\}$ with global polar coordinates (ρ, θ) so $\rho > 0$ and $\theta \in \mathbf{R}$. An *N-valued graph* on the annulus $D_s \setminus D_r$ is a single valued graph of a function u over $\{(\rho, \theta) \,|\, r < \rho \leq s\,,\, |\theta| \leq N\,\pi\}$.

In Theorem 1, we construct a sequence of disks $\Sigma_i \subset B_1 = B_1(0) \subset \mathbf{R}^3$ as above where the curvatures blow up only at 0 (see (1) and (2)) and $\Sigma_i \setminus \{x_3\text{-axis}\}$ consists of two multi-valued graphs for each i; see (3). Furthermore (see (4)), $\Sigma_i \setminus \{x_3 = 0\}$ converges to two embedded minimal disks $\Sigma^- \subset \{x_3 < 0\}$ and $\Sigma^+ \subset \{x_3 > 0\}$, each of which spirals into $\{x_3 = 0\}$ and thus is not proper; see Figure 2.

Received by the editors October 21, 2002.
2000 *Mathematics Subject Classification.* Primary 53A10, 49Q05.
The authors were partially supported by NSF Grants DMS 0104453 and DMS 0104187.

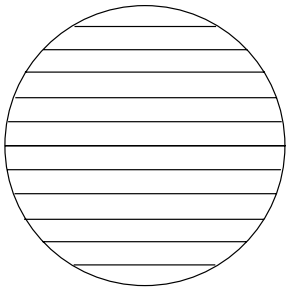

FIGURE 1. The limit in a ball of a sequence of degenerating helicoids is a foliation by parallel planes. This is smooth and proper.

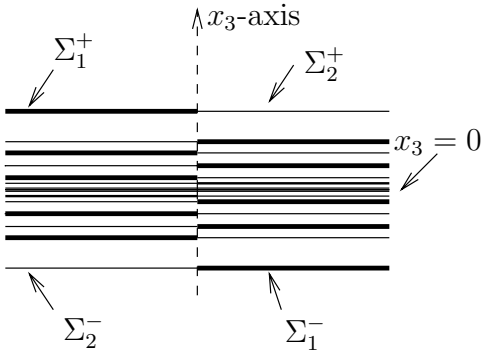

FIGURE 2. A schematic picture of the limit in Theorem 1 which is not smooth and not proper (the dotted x_3-axis is part of the limit). The limit contains four multi-valued graphs joined at the x_3-axis; Σ_1^+, Σ_2^+ above the plane $x_3 = 0$ and Σ_1^-, Σ_2^- below the plane. Each of the four spirals into the plane.

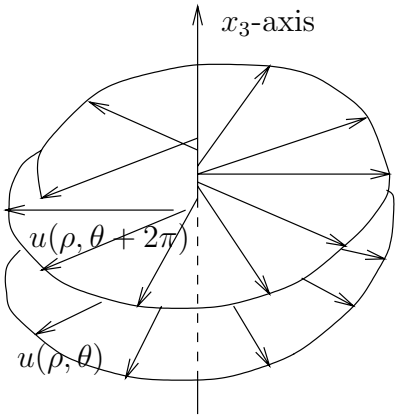

FIGURE 3. A multi-valued graph of a function u.

Theorem 1. *There is a sequence of compact embedded minimal disks* $0 \in \Sigma_i \subset B_1 \subset \mathbf{R}^3$ *with* $\partial\Sigma_i \subset \partial B_1$ *and containing the vertical segment* $\{(0,0,t) \,|\, |t| < 1\} \subset \Sigma_i$*, and such that the following conditions are satisfied:*

(1) $\lim_{i\to\infty} |A_{\Sigma_i}|^2(0) = \infty$.
(2) $\sup_i \sup_{\Sigma_i \setminus B_\delta} |A_{\Sigma_i}|^2 < \infty$ *for all* $\delta > 0$.
(3) $\Sigma_i \setminus \{x_3\text{-}axis\} = \Sigma_{1,i} \cup \Sigma_{2,i}$ *for multi-valued graphs* $\Sigma_{1,i}$ *and* $\Sigma_{2,i}$.
(4) $\Sigma_i \setminus \{x_3 = 0\}$ *converges to two embedded minimal disks* $\Sigma^\pm \subset \{\pm x_3 > 0\}$ *with* $\overline{\Sigma^\pm} \setminus \Sigma^\pm = B_1 \cap \{x_3 = 0\}$. *Moreover,* $\Sigma^\pm \setminus \{x_3\text{-}axis\} = \Sigma_1^\pm \cup \Sigma_2^\pm$ *for multi-valued graphs* $\Sigma_1^\pm$ *and* $\Sigma_2^\pm$ *each of which spirals into* $\{x_3 = 0\}$*; see Figure 2.*

It follows from (4) that $\Sigma_i \setminus \{0\}$ converges to a lamination of $B_1 \setminus \{0\}$ (with leaves Σ^-, Σ^+, and $B_1 \cap \{x_3 = 0\} \setminus \{0\}$) which does not extend to a lamination of B_1. Namely, 0 is not a removable singularity.

The multi-valued graphs that we will consider will never close up; in fact they will all be embedded. The most important example of an embedded minimal multi-valued graph comes from the helicoid. The *helicoid* is the minimal surface Σ in $\mathbf{R}^3$ parametrized by $(s\cos t, s\sin t, t)$, where s, $t \in \mathbf{R}$. Thus $\Sigma \setminus \{x_3\text{-axis}\} = \Sigma_1 \cup \Sigma_2$, where Σ_1, Σ_2 are ∞-valued graphs on $\mathbf{C} \setminus \{0\}$. Σ_1 is the graph of the function $u_1(\rho, \theta) = \theta$ and Σ_2 is the graph of the function $u_2(\rho, \theta) = \theta + \pi$.

We will use standard (x_1, x_2, x_3) coordinates on $\mathbf{R}^3$ and $z = x + i\,y$ on $\mathbf{C}$. Given $f : \mathbf{C} \to \mathbf{C}^n$, $\partial_x f$ and $\partial_y f$ denote $\frac{\partial f}{\partial x}$ and $\frac{\partial f}{\partial y}$, respectively; similarly, $\partial_z f = (\partial_x f - i\partial_y f)/2$. For $p \in \mathbf{R}^3$ and $s > 0$, the ball in $\mathbf{R}^3$ is $B_s(p)$. K_Σ is the sectional curvature of a smooth surface Σ. When Σ is immersed in $\mathbf{R}^3$, then A_Σ will be its second fundamental form (so when Σ is minimal, then $|A_\Sigma|^2 = -2\,\mathrm{K}_\Sigma$). When Σ is oriented, $\mathbf{n}_\Sigma$ is the unit normal.

1. Preliminaries on the Weierstrass representation

Let $\Omega \subset \mathbf{C}$ be a domain. The classical Weierstrass representation (see [Os]) starts from a meromorphic function g on Ω and a holomorphic one-form ϕ on Ω, and associates to them a (branched) conformal minimal immersion $F : \Omega \to \mathbf{R}^3$ by

$$F(z) = \mathrm{Re} \int_{\zeta \in \gamma_{z_0,z}} \left(\frac{1}{2}\,(g^{-1}(\zeta) - g(\zeta)), \frac{i}{2}\,(g^{-1}(\zeta) + g(\zeta)), 1 \right) \phi(\zeta)\,. \tag{1.1}$$

Here $z_0 \in \Omega$ is a fixed base point and the integration is along a path $\gamma_{z_0,z}$ from z_0 to z. The choice of z_0 changes F by adding a constant. We will assume that $F(z)$ does not depend on the choice of path $\gamma_{z_0,z}$; this is the case, for example, when g has no zeros or poles and Ω is simply connected.

The unit normal $\mathbf{n}$ and Gauss curvature K of the resulting surface are then (see sections 8, 9 in [Os])

$$\mathbf{n} = \left(2\,\mathrm{Re}\; g, 2\,\mathrm{Im}\; g, |g|^2 - 1\right)/(|g|^2 + 1)\,, \tag{1.2}$$

$$\mathrm{K} = -\left[\frac{4|\partial_z g|\,|g|}{|\phi|\,(1 + |g|^2)^2} \right]^2 . \tag{1.3}$$

Since the pullback $F^*(dx_3)$ is $\mathrm{Re}\;\phi$ by (1.1), ϕ is usually called the *height differential*. By (1.2), g is the composition of the Gauss map followed by stereographic projection.

To ensure that F is an immersion (i.e., $dF \neq 0$), we will assume that ϕ does not vanish and g has no zeros or poles. The two standard examples are

$$g(z) = z,\ \phi(z) = dz/z,\ \Omega = \mathbf{C} \setminus \{0\},\ \text{giving a catenoid}\,, \tag{1.4}$$

$$g(z) = \mathrm{e}^{iz},\ \phi(z) = dz,\ \Omega = \mathbf{C},\ \text{giving a helicoid}\,. \tag{1.5}$$

The next lemma records the differential of F.

Lemma 1. *If F is given by (1.1) with $g(z) = e^{i\,(u(z) + iv(z))}$ and $\phi = dz$, then*

$$\partial_x F = (\sinh v\,\cos u, \sinh v\,\sin u, 1)\,, \tag{1.6}$$

$$\partial_y F = (\cosh v\,\sin u, -\cosh v\,\cos u, 0)\,. \tag{1.7}$$

2. The proof of Theorem 1

To show Theorem 1, we first construct a one-parameter family (with parameter $a \in (0, 1/2)$) of minimal immersions F_a by making a specific choice of Weierstrass data $g = e^{ih_a}$ (where $h_a = u_a + i\, v_a$), $\phi = dz$, and domain Ω_a to use in (1.1). We show in Lemma 2 that this one-parameter family of immersions is compact. Lemma 3 shows that the immersions $F_a : \Omega_a \to \mathbf{R}^3$ are embeddings.

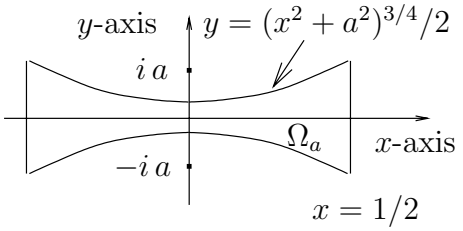

FIGURE 4. The domain Ω_a.

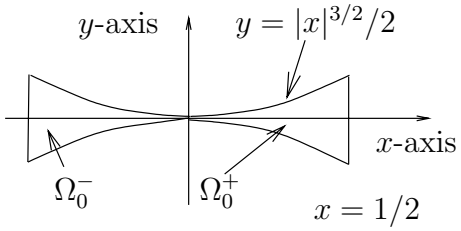

FIGURE 5. $\Omega_0 = \bigcap_{a>0} \Omega_a \setminus \{0\}$ and its two components Ω_0^+ and Ω_0^-.

For each $0 < a < 1/2$, set (see Figure 4)

$$h_a(z) = \frac{1}{a} \arctan\left(\frac{z}{a}\right) \text{ on } \Omega_a = \{(x,y) \,|\, |x| \leq 1/2,\, |y| \leq (x^2+a^2)^{3/4}/2\}\,. \tag{2.1}$$

Note that h_a is well-defined, since Ω_a is simply connected and $\pm i\, a \notin \Omega_a$. For future reference,

$$\partial_z h_a(z) = \frac{1}{z^2+a^2} = \frac{x^2+a^2-y^2-2i\,xy}{(x^2+a^2-y^2)^2+4x^2y^2}\,, \tag{2.2}$$

$$\mathrm{K}_a(z) = \frac{-|\partial_z h_a|^2}{\cosh^4 v_a} = \frac{-|z^2+a^2|^{-2}}{\cosh^4\left(\mathrm{Im}\,\arctan(z/a)/a\right)}\,. \tag{2.3}$$

Here (2.3) used (1.3). Note that, by the Cauchy-Riemann equations,

$$\partial_z h_a = (\partial_x - i\,\partial_y)(u_a + iv_a)/2 = \partial_x u_a - i\,\partial_y u_a = \partial_y v_a + i\,\partial_x v_a\,. \tag{2.4}$$

In the rest of this paper we let $F_a : \Omega_a \to \mathbf{R}^3$ be from (1.1) with $g = e^{i\,h_a}$, $\phi = dz$, and $z_0 = 0$. Set $\Omega_0 = \bigcap_a \Omega_a \setminus \{0\}$, so $\Omega_0 = \{(x,y) \,|\, 0 < |x| \leq 1/2,\, |y| \leq |x|^{3/2}/2\}$; see Figure 5. The family of functions h_a is not compact, since $\lim_{a\to 0} |h_a|(z) = \infty$ for $z \in \Omega_0$. However, the next lemma shows that the family of immersions F_a is compact.

Lemma 2. *If $a_j \to 0$, then there is a subsequence a_i for which F_{a_i} converges uniformly in C^2 on compact subsets of Ω_0.*

Proof. Since h_a and $-1/z$ are holomorphic and

$$|\partial_z h_a(z) - \partial_z(-1/z)| = a^2\,|z|^{-2}\,|z^2+a^2|^{-1}\,, \tag{2.5}$$

we get easily that ∇h_a converges as $a \to 0$ to $\nabla(-1/z)$ uniformly on compact subsets of Ω_0. Since each $v_a(x,0) = 0$, the fundamental theorem of calculus gives that the v_a's converge uniformly in C^1 on compact subsets of Ω_0. (Unfortunately, the u_a's do not converge.)

Let $\Omega_0^\pm = \{\pm x > 0\} \cap \Omega_0$ be the two components of Ω_0; see Figure 5. Set $b_j^+ = u_{a_j}(1/2)$ and $b_j^- = u_{a_j}(-1/2)$ and choose a subsequence a_i so both b_i^- and b_i^+

converge modulo 2π (this is possible since $T^2 = \mathbf{R}^2/(2\pi\mathbf{Z}^2)$ is compact). Arguing as above, we find that $h_{a_i} - b_i^{\pm}$ converges uniformly in C^1 on compact subsets of $\Omega_0^{\pm}$. Therefore, by Lemma 1, the minimal immersions corresponding to Weierstrass data $g = \mathrm{e}^{i(h_{a_i} - b_i^{\pm})}$, $\phi = dz$ converge uniformly in C^2 on compact subsets of $\Omega_0^{\pm}$ as $i \to \infty$. □

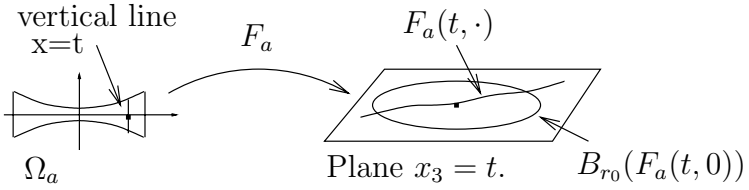

FIGURE 6. A horizontal slice in Lemma 3.

The main difficulty in proving Theorem 1 is showing that the immersions $F_a : \Omega_a \to \mathbf{R}^3$ are embeddings. This will follow easily from (A) and (B) below. Namely, we show in Lemma 3, see Figures 6 and 7, that for $|t| \le 1/2$:

(A) The horizontal slice $\{x_3 = t\} \cap F_a(\Omega_a)$ is the image of the vertical segment $\{x = t\}$ in the plane, i.e., $x_3(F_a(x,y)) = x$; see (2.6).

(B) The image $F_a(\{x = t\} \cap \Omega_a)$ is a graph over a line segment in the plane $\{x_3 = t\}$ (the line segment will depend on t); see (2.7).

(C) The boundary of the graph in (B) is outside the ball $B_{r_0}(F_a(t,0))$ for some $r_0 > 0$ and all a; see (2.8).

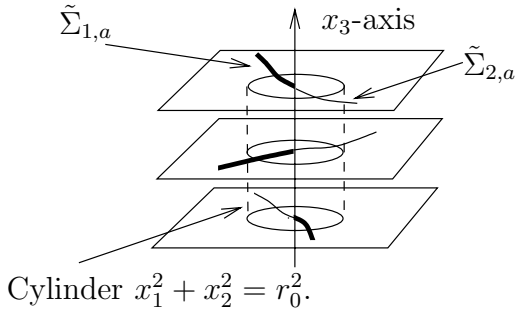

FIGURE 7. Horizontal slices of $F_a(\Omega_a)$ in Lemma 3.

Lemma 3.

$$x_3(F_a(x,y)) = x\,. \tag{2.6}$$

$$\textit{The curve } F_a(x,\cdot) : [-(x^2+a^2)^{3/4}/2, (x^2+a^2)^{3/4}/2] \to \{x_3 = x\} \textit{ is a graph}\,. \tag{2.7}$$

$$|F_a(x, \pm(x^2+a^2)^{3/4}/2) - F_a(x,0)| > r_0 \textit{ for some } r_0 > 0 \textit{ and all } a\,. \tag{2.8}$$

Proof. Since $z_0 = 0$ and $\phi = dz$, we get (2.6) from (1.1). Using $y^2 < (x^2 + a^2)/4$ on Ω_a, (2.2) and (2.4) give

$$|\partial_y u_a(x,y)| = \frac{2\,|xy|}{(x^2+a^2-y^2)^2 + 4x^2y^2} \leq \frac{4\,|xy|}{(x^2+a^2)^2}\,, \tag{2.9}$$

$$\partial_y v_a(x,y) = \frac{x^2+a^2-y^2}{(x^2+a^2-y^2)^2 + 4x^2y^2} > \frac{3}{8(x^2+a^2)}\,. \tag{2.10}$$

Set $y_{x,a} = (x^2+a^2)^{3/4}/2$. Integrating (2.9) gives

$$\max_{|y|\leq y_{x,a}} |u_a(x,y) - u_a(x,0)| \leq \int_0^{y_{x,a}} \frac{4|x|t}{(x^2+a^2)^2}\,dt = \frac{|x|}{2\,(x^2+a^2)^{1/2}} < 1\,. \tag{2.11}$$

Set $\gamma_{x,a}(y) = F_a(x,y)$. Since $v_a(x,0) = 0$ and $\cos(1) > 1/2$, combining (1.7) and (2.11) gives

$$\langle \gamma'_{x,a}(y), \gamma'_{x,a}(0)\rangle = \cosh v_a(x,y)\,\cos(u_a(x,y) - u_a(x,0)) > \cosh v_a(x,y)/2\,. \tag{2.12}$$

Here $\gamma'_{x,a}(y) = \partial_y F_a(x,y)$. By (2.12), the angle between $\gamma'_{x,a}(y)$ and $\gamma'_{x,a}(0)$ is always less than $\pi/2$; this gives (2.7). Since $v_a(x,0) = 0$, integrating (2.10) gives

$$\min_{y_{x,a}/2\leq|y|\leq y_{x,a}} |v_a(x,y)| \geq \int_0^{\frac{y_{x,a}}{2}} \frac{3\,dt}{8(x^2+a^2)} = \frac{3}{32(x^2+a^2)^{1/4}}\,. \tag{2.13}$$

Integrating (2.12) and using (2.13) gives

$$\langle \gamma_{x,a}(y_{x,a}) - \gamma_{x,a}(0), \gamma'_{x,a}(0)\rangle > \frac{(x^2+a^2)^{3/4}}{16}\,\mathrm{e}^{(x^2+a^2)^{-1/4}/11}\,. \tag{2.14}$$

Since $\lim_{s\to 0} s^3\,\mathrm{e}^{s^{-1}/11} = \infty$, (2.14) and its analog for $\gamma_{x,a}(-y_{x,a})$ give (2.8). □

Corollary 1. *See Figure 7. Let r_0 be given by* (2.8).

(i) *F_a is an embedding.*
(ii) *$F_a(t,0) = (0,0,t)$ for $|t| < 1/2$.*
(iii) *$\{0 < x_1^2 + x_2^2 < r_0^2\} \cap F_a(\Omega_a) = \tilde{\Sigma}_{1,a} \cup \tilde{\Sigma}_{2,a}$ for multi-valued graphs $\tilde{\Sigma}_{1,a}$, $\tilde{\Sigma}_{2,a}$ over $D_{r_0} \setminus \{0\}$.*

Proof. Equations (2.6) and (2.7) immediately give (i).

Since $z_0 = 0$, $F(0,0) = (0,0,0)$. Integrating (1.6) and using $v_a(x,0) = 0$ then gives (ii).

By (1.2), F_a is "vertical," i.e., $\langle \mathbf{n}, (0,0,1)\rangle = 0$, when $|g_a| = 1$. However, $|g_a(x,y)| = 1$ exactly when $y = 0$, so that, by (ii), the image is graphical away from the x_3-axis. Combining this with (2.8) gives (iii). □

Corollary 1 constructs the embeddings F_a that will be used in Theorem 1, and shows property (3). To prove Theorem 1, we need therefore only show (1), (2), and (4).

Proof of Theorem 1. By scaling, it suffices to find a sequence $\Sigma_i \subset B_R$ for some $R > 0$. Corollary 1 gives minimal embeddings $F_a : \Omega_a \to \mathbf{R}^3$ with $F_a(t,0) = (0,0,t)$ for $|t| < 1/2$, and so (3) holds for any $R \leq r_0$. Set $R = \min\{r_0/2, 1/4\}$ and $\Sigma_i = B_R \cap F_{a_i}(\Omega_{a_i})$, where the sequence a_i is to be determined.

To get (1), simply note that, by (2.3), $|\mathrm{K}_a|(0) = a^{-4} \to \infty$ as $a \to 0$.

We next show (2). First, by (2.3), $\sup_a \sup_{\{|x|\geq\delta\}\cap\Omega_a} |\mathrm{K}_a| < \infty$ for all $\delta > 0$. Combined with (3) and Heinz's curvature estimate for minimal graphs (i.e., 11.7 in [Os]), this gives (2).

To get (4), use Lemma 2 to choose $a_i \to 0$ so the mappings F_{a_i} converge uniformly in C^2 on compact subsets to $F_0 : \Omega_0 \to \mathbf{R}^3$. Hence, by Lemma 3, $\Sigma_i \setminus \{x_3 = 0\}$ converges to two embedded minimal disks $\Sigma^{\pm} \subset F_0(\Omega_0^{\pm})$ with $\Sigma^{\pm} \setminus \{x_3\text{-axis}\} = \Sigma_1^{\pm} \cup \Sigma_2^{\pm}$ for multi-valued graphs $\Sigma_j^{\pm}$. To complete the proof, we show that each graph $\Sigma_j^{\pm}$ is ∞-valued (and, hence, spirals into $\{x_3 = 0\}$). Note that, by (3) and (1.7), the level sets $\{x_3 = x\} \cap \Sigma_j^{\pm}$ are graphs over the line in the direction

$$\lim_{a \to 0} (\sin u_a(x,0), -\cos u_a(x,0), 0)\,. \tag{2.15}$$

Therefore, since an easy calculation gives, for $0 < t < 1/4$,

$$\lim_{a \to 0} |u_a(t,0) - u_a(2t,0)| = 1/(2t)\,, \tag{2.16}$$

we see that $\{t < |x_3| < 2t\} \cap \Sigma_j^{\pm}$ contains an embedded N_t-valued graph, where $N_t \approx 1/(4\pi t) \to \infty$ as $t \to 0$. It follows that $\Sigma_j^{\pm}$ must spiral into $\{x_3 = 0\}$, completing (4). □

References

[CM1] T.H. Colding and W.P. Minicozzi II, Embedded minimal disks, To appear in The Proceedings of the Clay Mathematics Institute Summer School on the Global Theory of Minimal Surfaces. MSRI. math.DG/0206146.

[CM2] ———, The space of embedded minimal surfaces of fixed genus in a 3-manifold IV; Locally simply connected, preprint, math.AP/0210119.

[Os] R. Osserman, A survey of minimal surfaces, *Dover*, 2nd. edition (1986). MR **87j:**53012

Courant Institute of Mathematical Sciences, 251 Mercer Street, New York, New York 10012 and Princeton University, Fine Hall, Washington Rd., Princeton, New Jersey 08544-1000

E-mail address: colding@cims.nyu.edu

Department of Mathematics, Johns Hopkins University, 3400 N. Charles St., Baltimore, Maryland 21218

E-mail address: minicozz@jhu.edu